

A Nonlinear Model Predictive Control Scheme for Cooperative Manipulation with Singularity and Collision Avoidance

Alexandros Nikou, Christos Verginis, Shahab Heshmati-alamdari and Dimos V.
Dimarogonas

Abstract

This paper addresses the problem of cooperative transportation of an object rigidly grasped by N robotic agents. In particular, we propose a Nonlinear Model Predictive Control (NMPC) scheme that guarantees the navigation of the object to a desired pose in a bounded workspace with obstacles, while complying with certain input saturations of the agents. Moreover, the proposed methodology ensures that the agents do not collide with each other or with the workspace obstacles as well as that they do not pass through singular configurations. The feasibility and convergence analysis of the NMPC are explicitly provided. Finally, simulation results illustrate the validity and efficiency of the proposed method.

Index Terms

Multi-Agent Systems, Cooperative control, Cooperative Manipulation, Nonlinear Model Predictive Control, Collision Avoidance.

Alexandros Nikou, Christos Verginis and Dimos V. Dimarogonas are with the ACCESS Linnaeus Center, School of Electrical Engineering, KTH Royal Institute of Technology, SE-100 44, Stockholm, Sweden and with the KTH Center for Autonomous Systems. Email: {anikou, cverginis, dimos}@kth.se. Shahab Heshmati-alamdari is with the Control Systems Lab, Department of Mechanical Engineering, National Technical University of Athens, 9 Heron Polytechniou Street, Zografou 15780, Athens, Greece. Email: {shahab}@mail.ntua.gr. This work was supported by the H2020 ERC Starting Grant BUCOPHSYS, the EU H2020 AEROWORKS project, the EU H2020 Co4Robots project, the Swedish Foundation for Strategic Research (SSF), the Swedish Research Council (VR) and the Knut och Alice Wallenberg Foundation (KAW).

I. INTRODUCTION

Over the last years, multi-agent systems have gained a significant amount of attention, due to the advantages they offer with respect to single-agent setups. In the case of robotic manipulation and object transportation, difficult tasks involving heavy payloads as well as challenging maneuvers necessitate the employment of multiple robots. Fig. 1 depicts a system of two robotic mobile manipulators (KUKA youBots), each comprising of a moving base and a robotic arm of 5 Degrees of Freedom (DOF).

Early works related to cooperative manipulation develop control architectures where the robotic agents communicate and share information with each other as well as completely decentralized schemes, where each agent uses only local information or observers, avoiding potential communication delays [1]–[7]. Impedance and force/motion control constitutes the most common methodology used in the related literature [1], [8]–[16]. However, most of the aforementioned works employ force/torque sensors to acquire knowledge of the manipulator-object contact forces/torques, which, however, may result to performance decline due to sensor noise or mounting difficulties. Recent technological advances allow to manipulator grippers to grasp rigidly certain objects (see e.g., [17]), which, as shown in this work, can render the use of force/torque sensors unnecessary.

Furthermore, in manipulation tasks, such as pose/force or trajectory tracking, collision with obstacles of the environment has been dealt with only by exploiting the extra degrees of freedom that appear in over-actuated robotic agents. Potential field-based algorithms may suffer from local minima and navigation functions [18] cannot be extended to multi-agent second order dynamical systems in a trivial way. Moreover, these methods usually result in high control input values near obstacles that need to be avoided, which might conflict the saturation of the actual motor inputs.

Another important property that concerns robotic manipulators is the singularities of the Jacobian matrix, which maps the joint velocities of the agent to a 6D vector of generalized velocities. Such *singular kinematic* configurations, that indicate directions towards which the agent cannot move, must be always avoided, especially when dealing with task-space control in the end-effector [19]. In the same vein, *representation* singularities can also occur in the mapping from coordinate rates to angular velocities of a rigid body.

In this work, we aim to address the problem of cooperative manipulation of an object in a



Fig. 1. Two ground vehicles (KUKA youBots) consisting of a moving base and a attached manipulator with 5 DOF.

bounded workspace with obstacles. In particular, given N agents that rigidly grasp an object, we design control inputs for the navigation of the object to a final pose, while avoiding inter-agent collisions as well as collisions with obstacles. Moreover, we take into account constraints that emanate from control input saturation as well kinematic and representation singularities.

For the design of a stabilizing feedback control law for each robot, such that the desired specifications are met, while satisfying constraints on the controls and the states, one would ideally look for a closed loop solution for the feedback law satisfying the constraints while optimizing the performance. However, typically the optimal feedback law cannot be found analytically, even in the unconstrained case, since it involves the solution of the corresponding Hamilton-Jacobi-Bellman partial differential equations. One approach to circumvent this problem is the repeated solution of an open-loop optimal control problem for a given state. The first part of the resulting open-loop input signal is implemented and the whole process is repeated. Control approaches using this strategy are referred to as Nonlinear Model Predictive Control (NMPC) (see e.g. [20]–[34]) which we aim to use in this work for the problem of the constraint cooperative manipulation of an object which is rigidly grasped by N agents. To the best of the authors' knowledge, this problem has not been addressed in the related literature.

The remainder of the paper is structured as follows. Section II provides preliminary background. The system dynamics and the formal problem statement are given in Section III. Section IV discusses the technical details of the solution and Section V is devoted to a simulation example. Finally, conclusions and future work are discussed in Section VI.

II. NOTATION AND PRELIMINARIES

The set of positive integers is denoted as \mathbb{N} and the real n -coordinate space, with $n \in \mathbb{N}$, as \mathbb{R}^n ; $\mathbb{R}_{\geq 0}^n$ and $\mathbb{R}_{> 0}^n$ are the sets of real n -vectors with all elements nonnegative and positive, respectively. The notation $\mathbb{R}_{\geq 0}^{n \times n}$ and $\mathbb{R}_{> 0}^{n \times n}$, with $n \in \mathbb{N}$, stands for positive semi-definite and positive definite matrices, respectively. Moreover, $\|x\|$ is the Euclidean norm of a vector $x \in \mathbb{R}^n$. Given a set S , we denote by $|S|$ its cardinality and by $S^N = S \times \cdots \times S$ its N -fold Cartesian product. Given the sets S_1, S_2 , the *set difference* and the *Minkowski addition* are denoted by \setminus, \oplus , respectively, and are defined by $S_1 \setminus S_2 = \{s : s \in S_1 \text{ and } s_2 \notin S_2\}$ and $S_1 \oplus S_2 = \{s_1 + s_2 : s_1 \in S_1, s_2 \in S_2\}$, respectively. The $n \times n$ identity matrix and the $n \times m$ matrix with zero entries, are denoted by $I_n, 0_{n \times m}$ and $\mathbb{1}_n$, respectively, with $n, m \in \mathbb{N}$. The largest singular value of matrix $A \in \mathbb{R}^{n \times m}$ is denoted as $\sigma_{\max}(A)$.

The vector connecting the origins of coordinate frames $\{A\}$ and $\{B\}$ expressed in frame $\{C\}$ coordinates in 3-D space is denoted as $p_{B/A}^C = [x_{B/A}, y_{B/A}, z_{B/A}]^\top \in \mathbb{R}^3$. Given $a \in \mathbb{R}^3$, $S(a)$ is the skew-symmetric matrix defined according to $S(a)b = a \times b$. We further denote as $\eta_{A/B} = [\phi_{A/B}, \theta_{A/B}, \psi_{A/B}]^\top \in \mathbb{T}^3 \subseteq \mathbb{R}^3$ the x - y - z Euler angles representing the orientation of frame $\{A\}$ with respect to frame $\{B\}$, with $\phi_{A/B}, \psi_{A/B} \in [-\pi, \pi]$ and $\theta_{A/B} \in [-\frac{\pi}{2}, \frac{\pi}{2}]$, where \mathbb{T}^3 is the 3-D torus; Moreover, $R_A^B \in SO(3)$ is the rotation matrix associated with the same orientation and $SO(3)$ is the 3-D rotation group. The angular velocity of frame $\{B\}$ with respect to $\{A\}$, expressed in frame $\{C\}$ coordinates, is denoted as $\omega_{B/A}^C \in \mathbb{R}^3$ and it holds that $\dot{R}_A^B = S(\omega_{B/A}^A)R_A^B$. We further define the sets $\mathbb{M} = \mathbb{R}^3 \times \mathbb{T}^3$, $\mathcal{N} = \{1, \dots, N\}$. We define also the set

$$\begin{aligned} \mathcal{O}_z &\triangleq \mathcal{O}(c_z, \beta_{1,z}, \beta_{2,z}, \beta_{3,z}) \\ &= \{p \in \mathbb{R}^3 : (p - c_z)^\top P(p - c_z) \leq 1\}, \end{aligned}$$

as the set of an *ellipsoid* in 3D, where $c_z \in \mathbb{R}^3$ is the center of the ellipsoid, $\beta_{1,z}, \beta_{2,z}, \beta_{3,z} \in \mathbb{R}_{> 0}$ the lengths of its three semi-axes and $z \geq 1$ is an index term. The eigenvector of matrix $P \in \mathbb{R}^3$ define the principal axes of the ellipsoid, and the eigenvalues of P are: $\beta_{1,z}^{-2}, \beta_{2,z}^{-2}$ and $\beta_{3,z}^{-2}$. For notational brevity, when a coordinate frame corresponds to an inertial frame of reference $\{I\}$, we will omit its explicit notation (e.g., $p_B = p_{B/I}^I, \omega_B = \omega_{B/I}^I, R_A = R_A^I$, etc.). Finally, all vector and matrix differentiations will be with respect to an inertial frame $\{I\}$, unless otherwise stated.

Definition 1. ([35]) A continuous function $f : [0, \alpha] \rightarrow \mathbb{R}_{\geq 0}$, $\alpha \in \mathbb{R}_{> 0}$ is said to belong to *class* \mathcal{K} , if is strictly increasing and $f(0) = 0$.

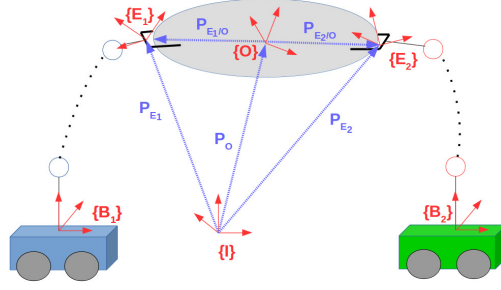


Fig. 2. Two robotic arms rigidly grasping an object with the corresponding frames.

Lemma 1. ([36]) *Let γ be a continuous, positive definite function and x be an absolutely continuous function on \mathbb{R} . If the following holds:*

- $\|x(\cdot)\| < \infty, \|\dot{x}(\cdot)\| < \infty,$
- $\lim_{t \rightarrow \infty} \int_0^t \gamma(x(s)) ds < \infty.$

Then, it holds that: $\lim_{t \rightarrow \infty} \|x(t)\| = 0.$

III. PROBLEM FORMULATION

Consider a bounded and convex workspace $\mathcal{W} \subseteq \mathbb{R}^3$ consisting of N robotic agents rigidly grasping an object, as shown in Fig. 2, and Z obstacles described by the ellipsoids $\mathcal{O}_z, z \in \mathcal{Z} = \{1, \dots, Z\}$. The free space is denoted as $\mathcal{W}_{\text{free}} = \mathcal{W} \setminus \bigcup_{z \in \mathcal{Z}} \mathcal{O}_z$. The agents are considered to be fully actuated and they consist of a base that is able to move around the workspace (e.g., mobile or aerial vehicle) and a robotic arm. The reference frames corresponding to the i -th end-effector and the object's center of mass are denoted with $\{E_i\}$ and $\{O\}$, respectively, whereas $\{I\}$ corresponds to an inertial reference frame. The rigidity of the grasps implies that the agents can exert any forces/torques along every direction to the object. We consider that each agent i knows the position and velocity only of its own state as well as its own and the object's geometric parameters. Moreover, no interaction force/torque measurements or on-line communication is required.

A. System model

1) *Robotic Agents:* We denote by $q_i : \mathbb{R}_{\geq 0} \rightarrow \mathbb{R}^{n_i}$ the joint space variables of agent $i \in \mathcal{N}$, with $n_i = n_{\alpha_i} + 6$, $q_i(t) = [p_{B_i}^\top(t), \eta_{B_i}^\top(t), \alpha_i^\top(t)]^\top$, where $p_{B_i} = [x_{B_i}, y_{B_i}, z_{B_i}]^\top : \mathbb{R}_{\geq 0} \rightarrow \mathbb{R}^3, \eta_{B_i} = [\phi_{B_i}, \theta_{B_i}, \psi_{B_i}]^\top : \mathbb{R}_{\geq 0} \rightarrow \mathbb{T}^3 \subseteq \mathbb{R}^3$ is the position and Euler-angle orientation of the agent's base,

and $\alpha_i : \mathbb{R}_{\geq 0} \rightarrow \mathbb{R}^{n_{\alpha_i}}, n_{\alpha_i} > 0$, are the degrees of freedom of the robotic arm. The overall joint space configuration vector is denoted as $q = [q_1^\top, \dots, q_N^\top]^\top \in \mathbb{R}^n$, with $n = \sum_{i \in \mathcal{N}} n_i$. In addition, we denote as $p_{E_i} : \mathbb{R}^{n_i} \rightarrow \mathbb{R}^3, \eta_{E_i} : \mathbb{R}^{n_i} \rightarrow \mathbb{T}^3 \subseteq \mathbb{R}^3$ the position and Euler-angle orientation of agent i 's end-effector. Let also $v_i : \mathbb{R}^{n_i} \times \mathbb{R}^{n_i} \rightarrow \mathbb{R}^6$ denote the velocity of agent i 's end-effector, with $v_i(q_i, \dot{q}_i) = [\dot{p}_{E_i}^\top, \omega_{E_i}^\top]^\top$, whereas $\dot{p}_{B_i}, \omega_{B_i} : \mathbb{R}^{n_i} \times \mathbb{R}^{n_i} \rightarrow \mathbb{R}^3$ are the linear and angular velocity, respectively, of the agent's base.

We consider that each agent $i \in \mathcal{N}$ has access to its own state q_i as well as $\dot{p}_{B_i}^{B_i}, \omega_{B_i}^{B_i}$, and $\dot{\alpha}_i$ via on-board sensors. Then, $\dot{p}_{B_i}, \omega_{B_i}$ can be obtained via $\dot{p}_{B_i} = R_{B_i}(\eta_{B_i})\dot{p}_{B_i}^{B_i}, \omega_{B_i} = R_{B_i}(\eta_{B_i})\omega_{B_i}^{B_i}$, where $R_{B_i} : \mathbb{T}^3 \rightarrow SO(3)$ is the rotation matrix of the agent i 's base. Moreover, $\dot{\eta}_{B_i}$ is related to ω_{B_i} via $\omega_{B_i} = J_{B_i}(\eta_{B_i})\dot{\eta}_{B_i}$, where $J_{B_i} : \mathbb{T}^3 \rightarrow \mathbb{R}^{3 \times 3}$, with

$$J_{B_i}(\eta_{B_i}) = \begin{bmatrix} 1 & 0 & \sin(\theta_{B_i}) \\ 0 & \cos(\phi_{B_i}) & -\cos(\theta_{B_i})\sin(\phi_{B_i}) \\ 0 & \sin(\phi_{B_i}) & \cos(\theta_{B_i})\cos(\phi_{B_i}) \end{bmatrix}.$$

The pose of the i th end-effector can be computed via

$$\begin{aligned} p_{E_i}(q_i) &= p_{B_i} + R_{B_i}(\eta_{B_i})k_{p_i}(\alpha_i), \\ \eta_{E_i}(q_i) &= k_{\eta_i}(\eta_{B_i}, \alpha_i), \end{aligned}$$

where $k_{p_i} : \mathbb{R}^{n_{\alpha_i}} \rightarrow \mathbb{R}^3, k_{\eta_i} : \mathbb{T}^3 \times \mathbb{R}^{n_{\alpha_i}} \rightarrow \mathbb{T}^3$ are the forward kinematics of the robotic arm [19]. Then, v_i can be computed as

$$\begin{aligned} v_i(q_i, \dot{q}_i) &= \begin{bmatrix} \dot{p}_{E_i}(q_i, \dot{q}_i) \\ \omega_{E_i}(q_i, \dot{q}_i) \end{bmatrix} \\ &= \begin{bmatrix} \dot{p}_{B_i} - S(R_{B_i}k_{p_i})\omega_{B_i} + R_{B_i}\frac{\partial k_{p_i}}{\partial \alpha_i} \\ \omega_{B_i} + R_{B_i}J_{A_i}\dot{\alpha}_i \end{bmatrix}, \end{aligned} \quad (1)$$

where $J_{A_i} : \mathbb{R}^{n_{\alpha_i}} \rightarrow \mathbb{R}^{3 \times n_{\alpha_i}}$ is the angular Jacobian of the robotic arm with respect to the agent's base. The differential kinematics (1) can be written as

$$v_i(q_i, \dot{q}_i) = \begin{bmatrix} \dot{p}_{E_i}(q_i, \dot{q}_i) \\ \omega_{E_i}(q_i, \dot{q}_i) \end{bmatrix} = J_i(q_i)\dot{q}_i, \quad (2)$$

where $J_i : \mathbb{R}^{n_i} \rightarrow \mathbb{R}^{6 \times n_i}$ is the agent Jacobian matrix, with

$$J_i(q_i) = \begin{bmatrix} I_3 & -S(R_{B_i}(\eta_{B_i})k_{p_i}(\alpha_i))J_{B_i}(\eta_{B_i}) & R_{B_i}(\eta_{B_i})\frac{\partial k_{p_i}(\alpha_i)}{\partial \alpha_i} \\ 0_{3 \times 3} & J_{B_i}(\eta_{B_i}) & R_{B_i}(\eta_{B_i})J_{A_i}(q_i) \end{bmatrix}.$$

Remark 1. Note that J_{B_i} becomes singular at representation singularities, when $\theta_{B_i} = \pm \frac{\pi}{2}$ and J_i becomes singular at kinematic singularities defined by the set

$$\mathcal{Q}_i = \{q_i \in \mathbb{R}^{n_i} : \det(J_i^\top J_i) = 0\}, i \in \mathcal{N}.$$

In the following, we will aim at guaranteeing that q_i will always be in the closed set:

$$\tilde{\mathcal{Q}}_i = \{q_i \in \mathbb{R}^{n_i} : |\det(J_i^\top J_i)| \geq \varepsilon > 0\}, i \in \mathcal{N},$$

for a small positive constant ε .

The joint-space dynamics for agent $i \in \mathcal{N}$ can be computed using the Lagrangian formulation:

$$B_i(q_i)\ddot{q}_i + N_i(q_i, \dot{q}_i)\dot{q}_i + g_{q_i}(q_i) = \tau_i - J_i^\top \lambda_i, \quad (3)$$

where $B_i : \mathbb{R}^{n_i} \rightarrow \mathbb{R}^{n_i \times n_i}$ is the joint-space positive definite inertia matrix, $N_i : \mathbb{R}^{n_i} \times \mathbb{R}^{n_i} \rightarrow \mathbb{R}^{n_i \times n_i}$ represents the joint-space Coriolis matrix, $g_{q_i} : \mathbb{R}^{n_i} \rightarrow \mathbb{R}^{n_i}$ is the joint-space gravity vector, $\lambda_i \in \mathbb{R}^6$ is the generalized force vector that agent i exerts on the object and $\tau_i \in \mathbb{R}^{n_i}$ is the vector of generalized joint-space inputs, with $\tau_i = [\lambda_{B_i}^\top, \tau_{\alpha_i}^\top]^\top$, where $\lambda_{B_i} = [f_{B_i}^\top, \mu_{B_i}^\top]^\top \in \mathbb{R}^6$ is the generalized force vector on the center of mass of the agent's base and $\tau_{\alpha_i} \in \mathbb{R}^{n_{\alpha_i}}$ is the torque inputs of the robotic arms' joints. By inverting (3) and using (2) and its derivative, we can obtain the task-space agent dynamics [19]:

$$M_i(q_i)\dot{v}_i + C_i(q_i, \dot{q}_i)v_i + g_i(q_i) = u_i - \lambda_i, \quad (4)$$

with the corresponding task-space terms:

$$\begin{aligned} M_i(q_i) &= [J_i(q_i)B_i^{-1}(q_i)J_i^\top(q_i)]^{-1}, \\ C_i(q_i, \dot{q}_i)J_i(q_i)\dot{q}_i &= M_i(q_i) \left[J_i(q_i)B_i^{-1}(q_i)N_i - \dot{J}_i(q_i) \right] \dot{q}_i, \\ g_i(q_i) &= M_i(q_i)J_i(q_i)B_i^{-1}(q_i)g_{q_i}(q_i). \end{aligned}$$

The task-space input wrench u_i can be translated to the joint space inputs $\tau_i \in \mathbb{R}^{n_i}$ via $\tau_i = J_i^\top(q_i)u_i + (I_{n_i} - J_i^\top(q_i)\bar{J}_i^\top(q_i))\tau_{i0}$, where \bar{J}_i is a generalized inverse of J_i [19]. The term τ_{i0} concerns over-actuated agents and does not contribute to end-effector forces.

We define by $\mathcal{A}_i(q_i) \triangleq \mathcal{O}_i, i \in \mathcal{N}$, the ellipsoid that bounds the i th agent's volume with the corresponding centers c_i and semi-axes $\beta_{i,1}, \beta_{i,2}, \beta_{i,3}$, i.e., the workspace of the arm of agent i [19] enlarged so that it includes the i th base. Note that \mathcal{A}_i depends on q_i and can be explicitly found.

2) *Object Dynamics*: Regarding the object, we denote as $x_o : \mathbb{R}_{\geq 0} \rightarrow \mathbb{M}$, $v_o : \mathbb{R}_{\geq 0} \rightarrow \mathbb{R}^6$ the pose and velocity of the object's center of mass, with $x_o(t) = [p_o^\top(t), \eta_o^\top(t)]^\top$, $p_o(t) = [x_o(t), y_o(t), z_o(t)]^\top$, $\eta_o(t) = [\phi_o(t), \theta_o(t), \psi_o(t)]^\top$ and $v_o(t) = [\dot{p}_o^\top(t), \omega_o^\top(t)]^\top$. The second order dynamics of the object are given by:

$$\dot{x}_o(t) = J_{o_r}^{-1}(x_o)v_o(t), \quad (5a)$$

$$\lambda_o = M_o(x_o)\dot{v}_o(t) + C_o(x_o, v_o)v_o(t) + g_o(x_o), \quad (5b)$$

where $M_o : \mathbb{M} \rightarrow \mathbb{R}^{6 \times 6}$ is the positive definite inertia matrix, $C_o : \mathbb{M} \times \mathbb{R}^6 \rightarrow \mathbb{R}^{6 \times 6}$ is the Coriolis matrix, $g_o : \mathbb{M} \rightarrow \mathbb{R}^6$ is the gravity vector, which are derived from the Newton-Euler formulation. In addition, $J_{o_r} : \mathbb{M} \rightarrow \mathbb{R}^{6 \times 6}$ is the object representation Jacobian $J_{o_r}(x_o) = \text{diag}\{I_3, J_{o_r, \theta}(x_o)\}$, with

$$J_{o_r, \theta}(x_o) = \begin{bmatrix} 1 & 0 & \sin(\theta_o) \\ 0 & \cos(\phi_o) & -\cos(\theta_o)\sin(\phi_o) \\ 0 & \sin(\phi_o) & \cos(\theta_o)\cos(\phi_o) \end{bmatrix},$$

which is singular when $\theta_o = \pm \frac{\pi}{2}$. Finally, $\lambda_o \in \mathbb{R}^6$ is the force vector acting on the object's center of mass. Also, similarly to the robotic agents, we define by $\mathcal{C}_o(x_o) \triangleq \mathcal{O}_o$, as the bounding ellipsoid of the object.

3) *Coupled Dynamics*: Consider N robotic agents rigidly grasping an object. Then, the coupled system object-agents behaves like a closed-chain robot and we can express the object's pose and velocity as a function of q_i and \dot{q}_i , $\forall i \in \mathcal{N}$. In view of Fig. 2, we have that

$$\begin{aligned} p_{E_i}(q_i(t)) &= p_o(t) + p_{E_i/O}(q_i) \\ &= p_o(t) + R_{E_i}(t)p_{E_i/O}^{E_i}, \end{aligned} \quad (6a)$$

$$\eta_{E_i}(q_i(t)) = \eta_o(t) + \eta_{E_i/O}, \quad (6b)$$

$\forall i \in \mathcal{N}$, where $p_{E_i/O}^{E_i}$ represents the constant distance and $\eta_{E_i/O}$ the relative orientation offset between the i th agent's end-effector and the object's center of mass, which are considered known. The grasp rigidity implies that $\omega_{E_i} = \omega_o$, $\forall i \in \mathcal{N}$. Therefore, by differentiating (6a), we obtain

$$v_i(q_i, \dot{q}_i(t)) = J_{o_i}(q_i)v_o(t), \quad (7)$$

which, by time differentiation, yields

$$\dot{v}_i(t) = J_{o_i}(q_i)\dot{v}_o(t) + \dot{J}_{o_i}(q_i)v_o(t), \quad (8)$$

where $J_{O_i} : \mathbb{R}^n \rightarrow \mathbb{R}^{6 \times 6}$ is a smooth mapping representing the Jacobian from the object to the i -th agent:

$$J_{O_i}(q_i) = \begin{bmatrix} I_3 & S(p_{O/E_i}(q_i)) \\ 0_{3 \times 3} & I_3 \end{bmatrix},$$

and is always full rank due to the grasp rigidity.

Remark 2. Since the geometric object parameters $p_{E_i/O}^{E_i}$ and $\eta_{E_i/O}$ are known, each agent can compute p_o, η_o and v_o simply by inverting (6) and (7), respectively, without employing any sensory data. In the same vein, all agents can also compute the object's bounding ellipsoid \mathcal{C}_o , which depends on q .

The Kineto-statics duality [19] along with the grasp rigidity suggest that the force λ_o acting on the object center of mass and the generalized forces $\lambda_i, i \in \mathcal{N}$, exerted by the agents at the contact points are related through

$$\lambda_o = G^\top(q)\bar{\lambda}, \quad (9)$$

where $\bar{\lambda} = [\lambda_1^\top, \dots, \lambda_N^\top]^\top \in \mathbb{R}^{6N}$ and $G : \mathbb{R}^n \rightarrow \mathbb{R}^{6N \times 6}$ is the grasp matrix, with $G(q) = [J_{O_1}^\top, \dots, J_{O_N}^\top]^\top$.

Next, we substitute (7) and (8) in (4) and we obtain in vector form after rearranging terms:

$$\bar{\lambda} = u - \bar{M}(q)G(q)\dot{v}_o - (\bar{M}(q)\dot{G}(q, \dot{q}) + \bar{C}(q, \dot{q})G(q))v_o - \bar{g}(q), \quad (10)$$

where we have used the stack forms $\bar{M} = \text{diag}\{[M_i]_{i \in \mathcal{N}}\}$, $\bar{C} = \text{diag}\{[C_i]_{i \in \mathcal{N}}\}$, $\bar{g} = [g_1^\top, \dots, g_N^\top]^\top$, and $u = [u_1^\top, \dots, u_N^\top]^\top$. By substituting (10) and (5) in (9) and by noticing from (6) that x_o depends on q owing to the grasp rigidity, we obtain the coupled dynamics:

$$\widetilde{M}(q)\dot{v}_o + \widetilde{C}(q, \dot{q})v_o + \widetilde{g}(q) = G^\top(q)u, \quad (11)$$

where:

$$\widetilde{M}(q) = M_o(q) + G^\top(q)\bar{M}(q)G(q), \quad (12a)$$

$$\widetilde{C}(q, \dot{q}) = C_o(q) + G^\top(q)\bar{M}(q)\dot{G}(q, \dot{q}) + G^\top(q)\bar{C}(q)G(q), \quad (12b)$$

$$\widetilde{g}(q) = g_o(q) + G^\top(q)\bar{g}(q), \quad (12c)$$

Remark 3. Note that the agents dynamics under consideration hold for generic robotic agents comprising of a moving base and a robotic arm. Hence, the considered framework can be applied for mobile, aerial, or underwater manipulators.

We can now formulate the problem considered in this work:

Problem 1. Consider N robotic agents rigidly grasping an object, governed by the coupled dynamics (11). Given the desired pose $x_{o,\text{des}}$, design the control input $u : \mathbb{R}_{\geq 0} \rightarrow \mathbb{R}^{6N}$ such that $\lim_{t \rightarrow \infty} x_o(t) = x_{o,\text{des}}$, while ensuring the satisfaction of the following collision avoidance and singularity properties:

- 1) $\mathcal{A}_i(q_i) \cap \mathcal{O}_z = \emptyset, \forall i \in \mathcal{N}, z \in \mathcal{Z}$,
- 2) $\mathcal{C}_o(x_o) \cap \mathcal{O}_z = \emptyset, \forall z \in \mathcal{Z}$,
- 3) $\mathcal{A}_i(q_i) \cap \mathcal{A}_j(q_j) = \emptyset, \forall i, j \in \mathcal{N}, i \neq j$,
- 4) $-\frac{\pi}{2} < -\bar{\theta} \leq \theta_o \leq \bar{\theta} < \frac{\pi}{2}$,
- 5) $-\frac{\pi}{2} < -\bar{\theta} \leq \theta_{B_i} \leq \bar{\theta} < \frac{\pi}{2}$,
- 6) $q_i \in \tilde{\mathcal{Q}}_i$.

for a $0 < \bar{\theta} < \frac{\pi}{2}$, as well as the input and velocity magnitude and input constraints: $|\tau_{i_k}| \leq \bar{\tau}_i, |\dot{q}_{i_k}| \leq \bar{q}_i, \forall k \in \{1, \dots, n_i\}, i \in \mathcal{N}$, for some positive constants $\bar{\tau}_i, \bar{q}_i, i \in \mathcal{N}$.

The aforementioned constraints correspond to the following specifications:

- 1) stands for collision avoidance between the agents and the obstacles.
- 2) stands for collision avoidance between the object and the obstacles.
- 3) stands for collision avoidance between the agents.
- 4) stands for representation singularity avoidance of the object.
- 5) stands for representation singularity avoidance of the agents' bases.
- 6) stands for kinematic singularity avoidance of the agents.

In order to solve the aforementioned problem, we need the following reasonable assumption regarding the workspace:

Assumption 1. (Problem Feasibility Assumption) The distance between any pair of obstacles is sufficiently large such that the coupled system object-agents can navigate among them without collisions.

We also define the following sets for every $i \in \mathcal{N}$:

$$S_{i,o}(q) = \{q_i \in \mathbb{R}^{n_i} : \mathcal{A}_i(q_i) \cap \mathcal{O}_z \neq \emptyset, \forall z \in \mathcal{Z}\},$$

$$S_{i,A}(q) = \{q_i \in \mathbb{R}^{n_i} : \mathcal{A}_i(q_i) \cap \mathcal{A}_j(q_j) \neq \emptyset, \forall j \in \mathcal{N} \setminus \{i\}\},$$

$$S_o(x_o) = \{x_o \in \mathbb{M} : \mathcal{C}_o(x_o) \cap \mathcal{O}_z \neq \emptyset\}.$$

associated with the desired collision-avoidance properties.

IV. PROBLEM SOLUTION

In this section, a systematic solution to Problem 1 is introduced. Our overall approach builds on designing a Nonlinear Model Predictive control scheme the system of the manipulators and the object. Nonlinear Model Predictive Control (see e.g. [20]–[28]) have been proven suitable for dealing with nonlinearities and state and input constraints.

The coupled agents-object *nonlinear dynamics* can be written in compact form as follows:

$$\dot{x} = f(x, u) = \begin{bmatrix} f_1(x, u) \\ f_2(x, u) \\ f_3(x, u) \end{bmatrix}, x(0) = x_0, \quad (13)$$

where $x = [x_o^\top, v_o^\top, q^\top]^\top \in \mathbb{R}^{n+12}$, $u \in \mathbb{R}^{6N}$ and

$$\begin{aligned} f_1(x, u) &= J_{O_r}^{-1}(x_o)v_o, \\ f_2(x, u) &= \widetilde{M}^{-1}(q) \left[G^\top(q)u - \widetilde{C}(q, \dot{q})v_o - \widetilde{g}(q) \right], \\ f_3(x, u) &= \hat{J}(q)J_o(q)\widetilde{I}v_o, \end{aligned}$$

where we have also used that:

$$\begin{aligned} \hat{J}(q) &= \text{diag} \left\{ [(J_i^\top J_i)^{-1} J_i^\top]_{i \in \mathcal{N}} \right\} \in \mathbb{R}^{n \times 6N}, \\ J_o(q) &= \text{diag} \left\{ [J_{o_i}]_{i \in \mathcal{N}} \right\} \in \mathbb{R}^{6N \times 6N}, \\ \widetilde{I} &= [I_6, \dots, I_6]^\top \in \mathbb{R}^{6N \times 6}. \end{aligned} \quad (14)$$

The expression for $f_3(x, u)$ is derived by employing (8) and (2). Note that f is *locally Lipschitz continuous* in its domain since it is continuously differentiable in its domain. Next, we define the respective errors:

$$e(t) = x(t) - x_{\text{des}} = \begin{bmatrix} x_o(t) \\ v_o(t) \\ q(t) \end{bmatrix} - \begin{bmatrix} x_{o,\text{des}} \\ \dot{x}_{o,\text{des}} \\ q_{\text{des}} \end{bmatrix} = \begin{bmatrix} x_o(t) - x_{o,\text{des}} \\ v_o(t) \\ q(t) - q_{\text{des}} \end{bmatrix} \in \mathbb{R}^{n+12}, \quad (15)$$

where $q_{\text{des}} = [q_{1,\text{des}}, \dots, q_{N,\text{des}}]^\top$ is appropriately chosen such that $x_o(t) = x_{o,\text{des}}, \forall t$ s.t. $q(t) = q_{\text{des}}$ (see (6)), and $\dot{x}_{o,\text{des}} = \dot{q}_{\text{des}} = 0$. The error dynamics are then $\dot{e}(t) = f(x(t), u(t))$, which can be appropriately transformed to be written as:

$$\dot{e}(t) = f_e(e(t), u(t)), e(0) = e_0 = x(0) - x_{\text{des}}. \quad (16)$$

where $f_e(t) \triangleq f(e(t) + x_{\text{des}}, u(t))$. By ignoring over-actuated input terms, we have that $\tau_i = J_i^\top(q_i)u_i$, which becomes

$$\|\tau_i\| \leq \bar{\tau}_i \Leftrightarrow \sigma_{\min,i}\|u_i\| \leq \bar{\tau}_i, \quad (17)$$

where we have employed the property $\sigma_{\min}(J_i^\top)\|u_i\| \leq \|J_i^\top u_i\|$, with $\sigma_{\min}(J_i^\top)$ denoting the minimum singular value of J_i^\top , which is strictly positive, if the constraint $q_i \in \tilde{\mathcal{Q}}_i$ is always satisfied. Hence, the constraint $|\tau_{i_k}| \leq \bar{\tau}_i$ is equivalent to

$$\|u_i\| \leq \frac{\bar{\tau}_i}{\sigma_{\min}(J_i^\top)}, \forall i \in \mathcal{N}. \quad (18)$$

Let us now define the following set $U \subseteq \mathbb{R}^{6N}$:

$$U = \left\{ u \in \mathbb{R}^{6N} : \|u_i\| \leq \frac{\bar{\tau}_i}{\sigma_{\min}(J_i^\top)}, \forall i \in \mathcal{N} \right\}, \quad (19)$$

as the set that captures the control input constraints of the error dynamics system (16). Define also the set $X \subseteq \mathbb{R}^{n+12}$:

$$X = \left\{ x \in \mathbb{R}^{n+12} : \theta_o(t) \in [-\bar{\theta}, \bar{\theta}], \theta_{B_i}(t) \in [-\bar{\theta}, \bar{\theta}], \right. \\ \left. |\dot{q}_{k_i}| \leq \bar{q}_i, q_i \in \tilde{\mathcal{Q}}_i \setminus (\mathcal{S}_{i,o}(q_i) \cup \mathcal{S}_{i,A}(q_i)), \right. \\ \left. x_o \in \mathbb{R}^3 \setminus \mathcal{S}_o(x_o), \forall t \in \mathbb{R}_{\geq 0} \right\}.$$

The set X captures all the state constraint of the system dynamics (13). In view of (15), we define the set $E \subseteq \mathbb{R}^{n+12}$ as:

$$E = \{e \in \mathbb{R}^{n+12} : e \in X \oplus (-x_{\text{des}})\},$$

as the set that captures all the constraints of the error dynamics system (16).

The problem in hand is the design of a control input $u(t) \in U$ such that $\lim_{t \rightarrow \infty} \|e(t)\| = 0$ while ensuring $e(t) \in E, \forall t \in \mathbb{R}_{\geq 0}$. In order to solve the aforementioned problem, we propose a Nonlinear Model Predictive scheme, that is presented hereafter.

Consider a sequence of sampling times $\{t_i\}_{i \geq 0}$ with a constant sampling period $0 < h < T_p$, where is T_p is the prediction horizon, such that:

$$t_{i+1} = t_i + h, \forall i \geq 0. \quad (20)$$

In the sampling-data NMPC, a finite-horizon open-loop optimal control problem (OCP) is solved at discrete sampling time instants t_i based on the current state error information $e(t_i)$. The solution is an optimal control signal $\hat{u}(t)$, for $t \in [t_i, t_i + T_p]$. For more details, the reader is referred

to [21]. The open-loop input signal applied in between the sampling instants is given by the solution of the following Optimal Control Problem (OCP):

$$\begin{aligned} & \min_{\hat{u}(\cdot)} J(e(t_i), \hat{u}(\cdot)) \\ & = \min_{\hat{u}(\cdot)} \left\{ V(\hat{e}(t_i + T_p)) + \int_{t_i}^{t_i + T_p} [F(\hat{e}(s), \hat{u}(s))] ds \right\} \end{aligned} \quad (21a)$$

subject to:

$$\dot{\hat{e}}(s) = f_e(\hat{e}(s), \hat{u}(s)), \hat{e}(t_i) = e(t_i), \quad (21b)$$

$$\hat{e}(s) \in E, \hat{u}(s) \in U, s \in [t_i, t_i + T_p], \quad (21c)$$

$$\hat{e}(t_i + T_p) \in \mathcal{E}_f, \quad (21d)$$

where the hat $\hat{\cdot}$ denotes the predicted variables (internal to the controller), i.e. $\hat{e}(\cdot)$ is the solution of (21b) driven by the control input $\hat{u}(\cdot) : [t_i, t_i + T_p] \rightarrow \mathcal{U}$ with initial condition $e(t_i)$. Note that the predicted values are not necessarily the same with the actual closed-loop values (see [21]). The term $F : E \times U \rightarrow \mathbb{R}_{\geq 0}$, is the *running cost*, and is chosen as:

$$F(e, u) = e^\top Q e + u^\top R u. \quad (22)$$

The terms $V : E \rightarrow \mathbb{R}_{> 0}$ and \mathcal{E}_f are the *terminal penalty cost* and *terminal set*, respectively, and are used to enforce the stability of the system (see Section 4.2). The terminal cost is given by $V(e) = e^\top P e$. The terms $Q \in \mathbb{R}_{\geq 0}^{(n+12) \times (n+12)}$, $P \in \mathbb{R}_{> 0}^{(n+12) \times (n+12)}$ and $R \in \mathbb{R}_{> 0}^{6N \times 6N}$ are chosen as:

$$Q = \text{diag}\{\tilde{q}_1, \dots, \tilde{q}_{n+12}\}, P = \text{diag}\{\tilde{p}_1, \dots, \tilde{p}_{n+12}\}, R = \text{diag}\{\tilde{r}_1, \dots, \tilde{r}_{6N}\}.$$

where $\tilde{q}_i \in \mathbb{R}_{\geq 0}$, $\tilde{p}_i \in \mathbb{R}_{> 0}$, $\forall i \in \{1, \dots, n + 12\}$ and $\tilde{r}_j \in \mathbb{R}_{> 0}$, $\forall j \in \{1, \dots, 6N\}$ are constant weights.

Lemma 2. *There exist functions $\alpha_1, \alpha_2 \in \mathcal{K}_\infty$ such that:*

$$\alpha_1(\|z\|) \leq F(e, u) \leq \alpha_2(\|z\|),$$

for every $z \triangleq [e^\top, u^\top]^\top \in \mathcal{E} \times \mathcal{U}$.

Proof. The proof can be found in Appendix A. □

The solution of the OCP (21a)-(21d) at time t_i provides an optimal control input denoted by $\hat{u}^*(t; e(t_i))$, for $t \in [t_i, t_i + T_p]$. It defines the open-loop input that is applied to the system until the next sampling instant t_{i+1} :

$$u(t; e(t_i)) = \hat{u}^*(t; e(t_i)), t \in [t_i, t_{i+1}). \quad (23)$$

The corresponding *optimal value function* is given by:

$$J^*(e(t_i)) \triangleq J^*(e(t_i), \hat{u}^*(\cdot; e(t_i))). \quad (24)$$

where $J(\cdot)$ as is given in (21a). The control input $u(t; e(t_i))$ is a feedback, since it is recalculated at each sampling instant using the new state information. The solution of (16) starting at time t_1 from an initial condition $e(t_1)$, applying a control input $u : [t_1, t_2] \rightarrow \mathcal{U}$ is denoted by $e(s; u(\cdot), e(t_1))$, $s \in [t_1, t_2]$. The predicted state of the system (16) at time $t_i + s$, $s > 0$ is denoted by $\hat{e}(t_i + s; u(\cdot), e(t_i))$ and it is based on the measurement of the state $e(t_i)$ at time t_i , when a control input $u(\cdot; e(t_i))$ is applied to the system (16) for the time period $[t_i, t_i + s]$. Thus, it holds that:

$$e(t_i) = \hat{e}(t_i; u(\cdot), e(t_i)). \quad (25)$$

We define an admissible control input as:

Definition 2. A control input $u : [0, T_p] \rightarrow \mathbb{R}^{6N}$ for a state e_0 is called *admissible*, if all the following hold:

- 1) $u(\cdot)$ is piecewise continuous;
- 2) $u(s) \in U, \forall s \in [0, T_p]$;
- 3) $e(s; u(\cdot), e_0) \in E, \forall s \in [0, T_p]$;
- 4) $e(T_p; u(\cdot), e_0) \in \mathcal{E}_f$;

Lemma 3. *The terminal penalty function $V(\cdot)$ is Lipschitz continuous in \mathcal{E}_f , with Lipschitz constant $L_V = 2\varepsilon_0\sigma_{\max}(P)$, for all $e(t) \in \mathcal{E}_f$.*

Proof. The proof can be found in Appendix B. □

Through the following theorem, we guarantee the stability of the system which is the solution to Problem 1.

Theorem 1. *Consider the Assumptions 1,2. Suppose also that:*

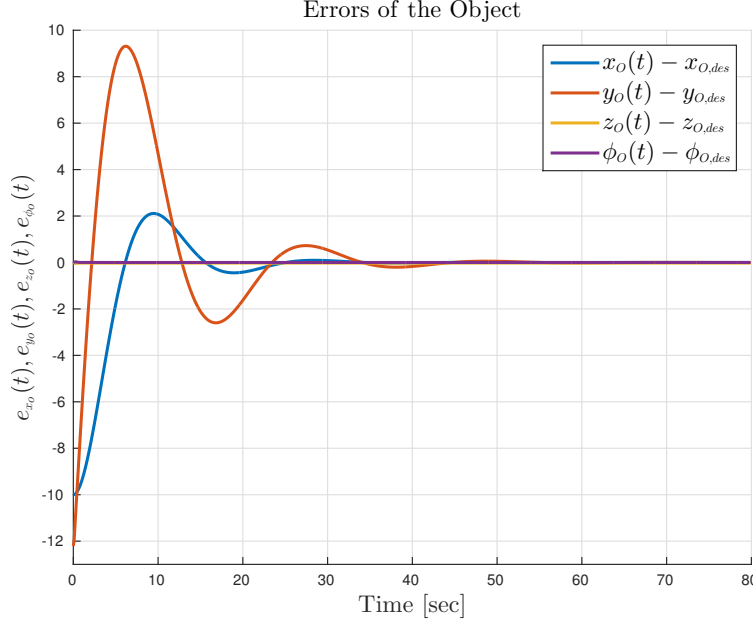


Fig. 3. The errors of the object.

- 1) The OCP (21a)-(21d) is feasible for the initial time $t = 0$.
- 2) The terminal set $\mathcal{E}_f \subseteq E$ is closed, with $0_{n+12} \in \mathcal{E}_f$.
- 3) The terminal set \mathcal{E}_f is chosen such that there exists an admissible control input $u_f : [0, h] \rightarrow \mathcal{U}$ such that for all $e(s) \in \mathcal{E}_f$ it holds that:
 - a) $e(s) \in \mathcal{E}_f, \forall s \in [0, h]$.
 - b) $\frac{\partial V}{\partial e} f_e(e(s), u_f(s)) + F(e(s), u_f(s)) \leq 0, \forall s \in [0, h]$.

Then, the closed loop trajectories of the system (16), converges to the set \mathcal{E}_f , as $t \rightarrow \infty$.

Proof. As usual in predictive control the proof consists of two parts: in the first part it is established that initial feasibility implies feasibility afterwards. Based on this result it is then shown that the error $e(t)$ converges to the terminal set \mathcal{E}_f . The feasibility analysis can be found in Appendix C. The convergence analysis can be found in D. \square

V. SIMULATION RESULTS

To demonstrate the efficiency of the proposed control protocol, we consider two simulation scenarios.

Scenario 1: Consider $N = 2$ ground vehicles equipped with 2 DOF manipulators, rigidly grasping an object with $n_1 = n_2 = 4, n = n_1 + n_2 = 8$. From (13) we have that $x =$

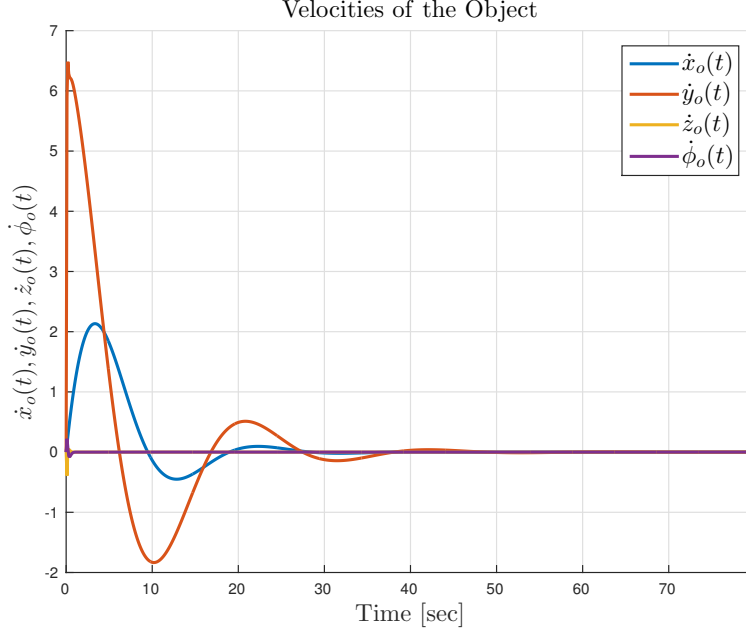


Fig. 4. The velocities of the object.

$[x_o^\top, v_o^\top, q^\top]^\top \in \mathbb{R}^{16}$, $u \in \mathbb{R}^8$, with $x_o = [p_o^\top, \phi_o]^\top \in \mathbb{R}^4$, $v_o = [\dot{p}_o^\top, \omega_{x_o}]^\top \in \mathbb{R}^4$, $p_o = [x_o, y_o, z_o]^\top \in \mathbb{R}^3$, $q = [q_1^\top, q_2^\top]^\top \in \mathbb{R}^8$, $q_i = [p_{B_i}^\top, \alpha_i^\top]^\top \in \mathbb{R}^4$, $p_{B_i} = [x_{B_i}, y_{B_i}]^\top \in \mathbb{R}^2$, $\alpha_i = [\alpha_{i_1}, \alpha_{i_2}]^\top \in \mathbb{R}^2$, $i \in \{1, 2\}$. The manipulators become singular when $\sin(\alpha_{i_1}) = 0$, $i \in \{1, 2\}$, thus the state constraints for the manipulators are set to:

$$\begin{aligned} \varepsilon < \alpha_{1_1} < \frac{\pi}{2} - \varepsilon, \quad -\frac{\pi}{2} + \varepsilon < \alpha_{1_2} < \frac{\pi}{2} - \varepsilon, \\ -\frac{\pi}{2} + \varepsilon < \alpha_{2_1} < -\varepsilon, \quad -\frac{\pi}{2} + \varepsilon < \alpha_{2_2} < \frac{\pi}{2} - \varepsilon. \end{aligned}$$

We also consider the input constraints:

$$-10 \leq u_{i,j}(t) \leq 10, i \in \{1, 2\}, j \in \{1, \dots, 4\}.$$

The initial conditions are set to:

$$\begin{aligned} x_o(0) &= \left[0, -2.2071, 0.9071, \frac{\pi}{2}\right]^\top, v_o(0) = [0, 0, 0, 0]^\top, \\ q_1(0) &= \left[0, 0, \frac{\pi}{4}, \frac{\pi}{4}\right]^\top, q_2(0) = \left[0, -4.4142, -\frac{\pi}{4}, -\frac{\pi}{4}\right]^\top. \end{aligned}$$

The desired goal states are set to:

$$\begin{aligned} x_{o,\text{des}} &= \left[10, 10, 0.9071, \frac{\pi}{2}\right]^\top, v_{o,\text{des}} = [0, 0, 0, 0]^\top, \\ q_{1,\text{des}} &= \left[10, 12.2071, \frac{\pi}{4}, \frac{\pi}{4}\right]^\top, q_{2,\text{des}} = \left[10, 7.7929, -\frac{\pi}{4}, -\frac{\pi}{4}\right]^\top. \end{aligned}$$

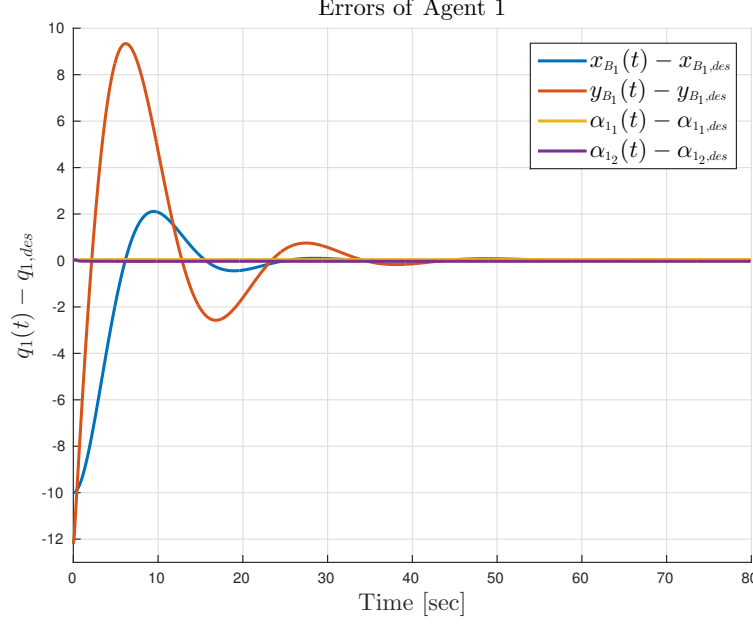


Fig. 5. The errors of vehicle 1 as well as the errors of the manipulator.

We set an obstacle between the initial and the desired pose of the object. the obstacle is spherical with center $[5, 5, 1]$ and radius 2. The sampling time is $h = 0.1$ sec, the horizon is set to $T_p = 0.3$ sec, and the total simulation time is 80 sec; The matrices P, Q, R are set to:

$$P = Q = 10I_{16 \times 16}, R = 2I_{8 \times 8}.$$

The simulation results are depicted in Fig. 3- Fig. 8, which shows that the states of the agents as well as the states of the object converge to the desired ones while guaranteeing that the obstacle is avoided and all state and input constraints are met.

Scenario 2: Consider $N = 3$ ground vehicles equipped with 2 DOF manipulators, rigidly grasping an object with $n_1 = n_2 = n_3 = 4, n = n_1 + n_2 + n_3 = 12$. From (13) we have that $x = [x_o^\top, v_o^\top, q^\top]^\top \in \mathbb{R}^{20}$, $u \in \mathbb{R}^{12}$, with $x_o = [p_o^\top, \phi_o]^\top \in \mathbb{R}^4$, $v_o = [\dot{p}_o^\top, \omega_{x_o}]^\top \in \mathbb{R}^4$, $p_o = [x_o, y_o, z_o]^\top \in \mathbb{R}^3$, $q = [q_1^\top, q_2^\top, q_3^\top]^\top \in \mathbb{R}^{12}$, $q_i = [p_{B_i}^\top, \alpha_i^\top]^\top \in \mathbb{R}^4$, $p_{B_i} = [x_{B_i}, y_{B_i}]^\top \in \mathbb{R}^2$, $\alpha_i = [\alpha_{i_1}, \alpha_{i_2}]^\top \in \mathbb{R}^2, i \in \{1, 2\}$. The manipulators become singular when $\sin(\alpha_{i_1}) = 0, i \in \{1, 2, 3\}$, thus the state constraints for the manipulators are set to:

$$\begin{aligned} \varepsilon < \alpha_{1_1} < \frac{\pi}{2} - \varepsilon, & -\frac{\pi}{2} + \varepsilon < \alpha_{1_2} < \frac{\pi}{2} - \varepsilon, \\ -\frac{\pi}{2} + \varepsilon < \alpha_{2_1} < -\varepsilon, & -\frac{\pi}{2} + \varepsilon < \alpha_{2_2} < \frac{\pi}{2} - \varepsilon. \end{aligned}$$

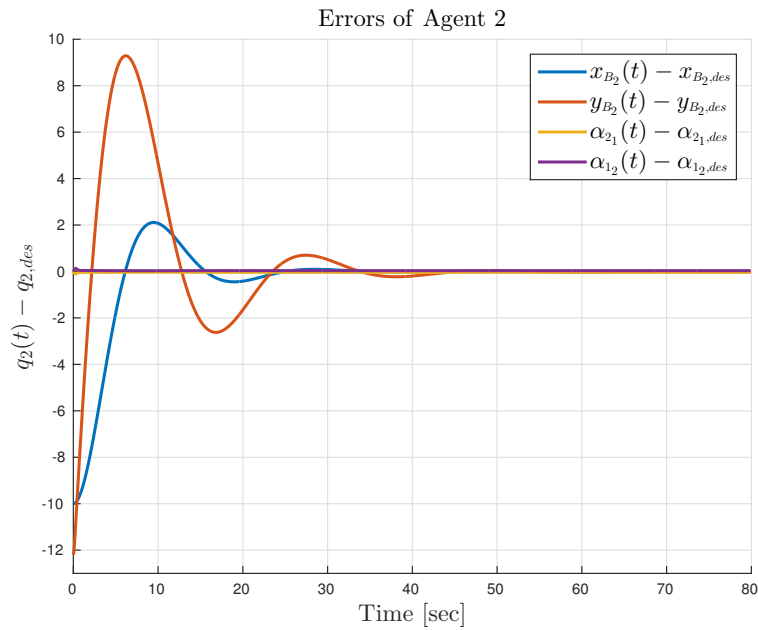


Fig. 6. The errors of vehicle 2 as well as the errors of the manipulator.

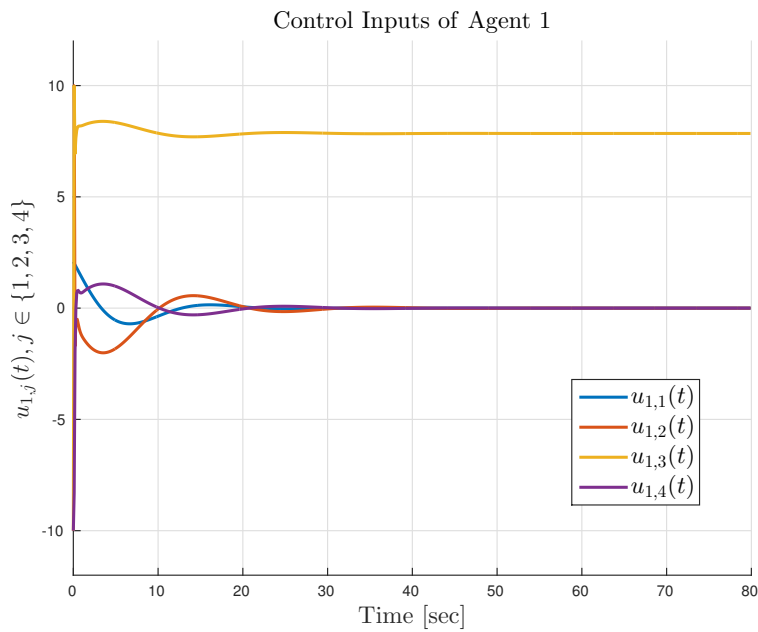


Fig. 7. The control inputs of the actuators of agent 1.

We also consider the input constraints:

$$-10 \leq u_{i,j}(t) \leq 10, i \in \{1, 2\}, j \in \{1, \dots, 4\}.$$

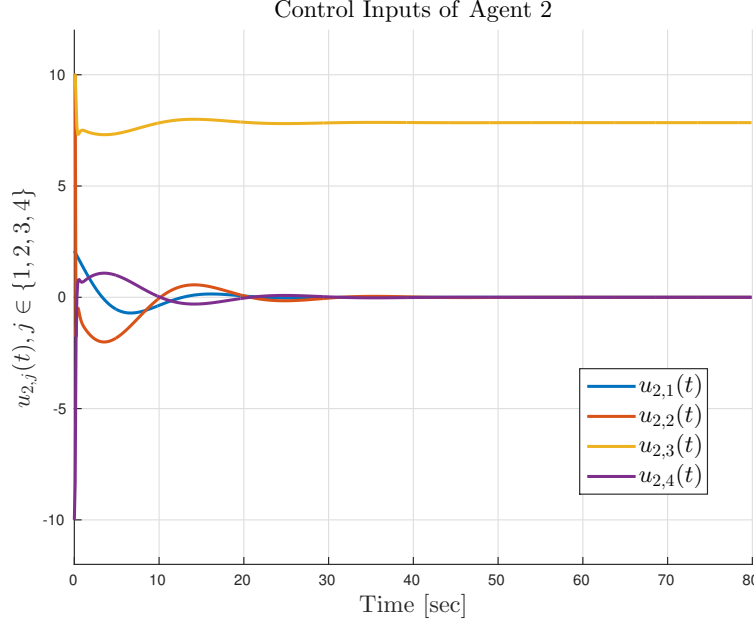


Fig. 8. The control inputs of the actuators of agent 2.

The initial conditions are set to:

$$\begin{aligned} x_o(0) &= \left[0, -2.2071, 0.9071, \frac{\pi}{2} \right]^\top, v_o(0) = [0, 0, 0, 0]^\top, \\ q_1(0) &= \left[0.5, 0, \frac{\pi}{4}, \frac{\pi}{4} \right]^\top, q_2(0) = \left[0, -4.4142, -\frac{\pi}{4}, -\frac{\pi}{4} \right]^\top, \\ q_3(0) &= \left[-0.5, 0, \frac{\pi}{4}, \frac{\pi}{4} \right]^\top. \end{aligned}$$

The desired goal states are set to:

$$\begin{aligned} x_{o,\text{des}} &= \left[5, -2.2071, 0.9071, \frac{\pi}{2} \right]^\top, v_{o,\text{des}} = [0, 0, 0, 0]^\top, \\ q_{1,\text{des}} &= \left[5.5, 0, \frac{\pi}{4}, \frac{\pi}{4} \right]^\top, q_{2,\text{des}} = \left[5, -4.4142, -\frac{\pi}{4}, -\frac{\pi}{4} \right]^\top, \\ q_{3,\text{des}} &= \left[4.5, 0.0, \frac{\pi}{4}, \frac{\pi}{4} \right]^\top. \end{aligned}$$

The sampling time is $h = 0.1$ sec, the horizon is set to $T_p = 0.5$ sec, and the total simulation time is 100 sec; The matrices P, Q, R are set to:

$$P = Q = 0.5I_{20 \times 20}, R = 0.5I_{12 \times 12}.$$

The simulation results are depicted in Fig. 9- Fig. 16, which shows that the states of the agents as well as the states of the object converge to the desired ones while guaranteeing that all state and

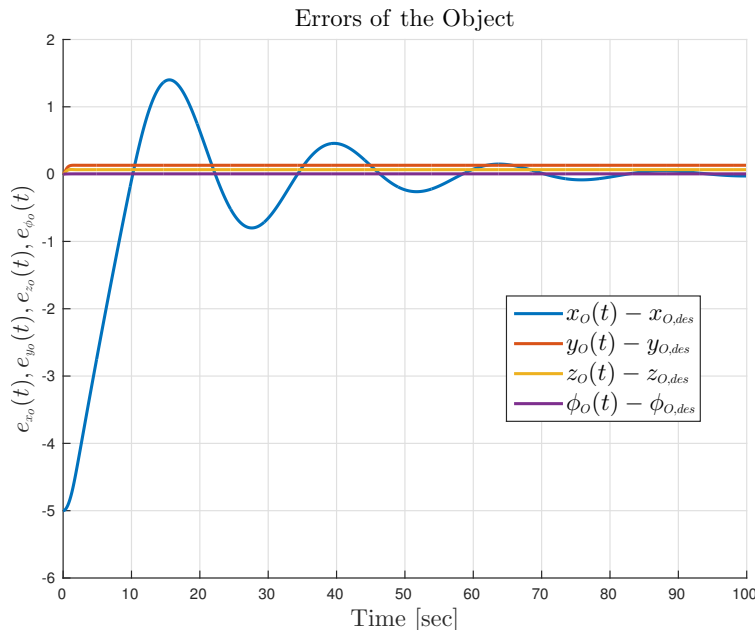


Fig. 9. The errors of the object.

input constraints are met. The simulation scenarios were carried out by using the NMPC toolbox given in [25] and they took 23500 sec, 45547 sec for Scenario 1 and Scenario 2, respectively, in MATLAB Environment on a desktop with 8 cores, 3.60 GHz SPU and 16GB of RAM.

VI. CONCLUSIONS AND FUTURE WORK

In this work we proposed a NMPC scheme for the cooperative transportation of an object rigidly grasped by N robotic agents. The proposed control scheme deals with singularities of the agents, inter-agent collision avoidance as well as collision avoidance between the agents and the object with the workspace obstacles. We proved the feasibility and convergence analysis of the proposed methodology and simulation results verified the efficiency of the approach. Future efforts will be devoted towards including load sharing coefficients, internal force regulation, and complete decentralization of the proposed method. Finally, we will try to decrease the overall complexity and carry out real-time experiments.

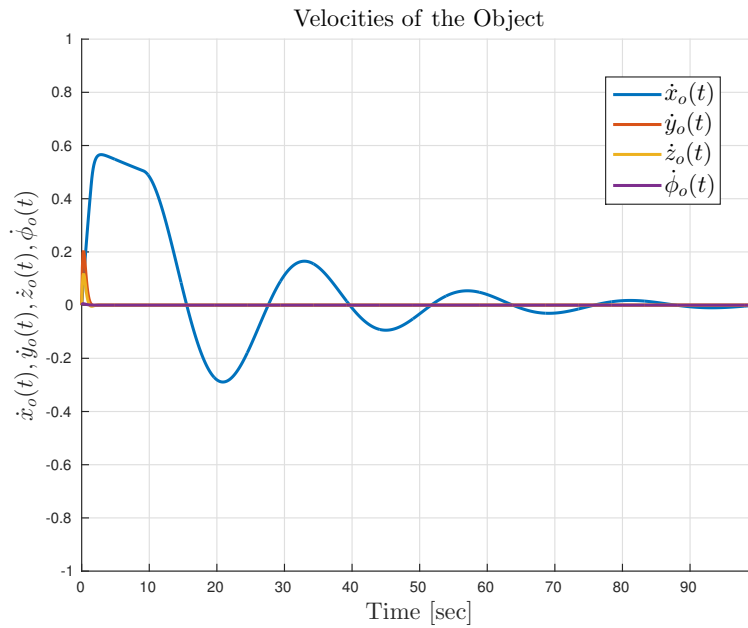


Fig. 10. The velocities of the object.

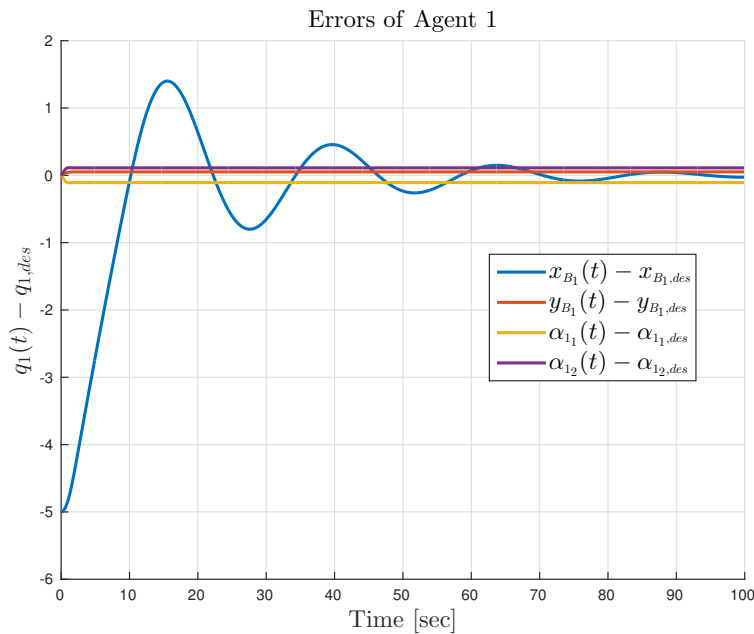


Fig. 11. The errors of vehicle 1 as well as the errors of the manipulator.

APPENDIX A

PROOF OF LEMMA 2

By invoking the fact that:

$$\lambda_{\min}(P)\|y\|^2 \leq y^\top P y \leq \lambda_{\max}(P)\|y\|^2, \forall y \in \mathbb{R}^n, P \in \mathbb{R}^{n \times n}, P = P^\top > 0, \quad (26)$$

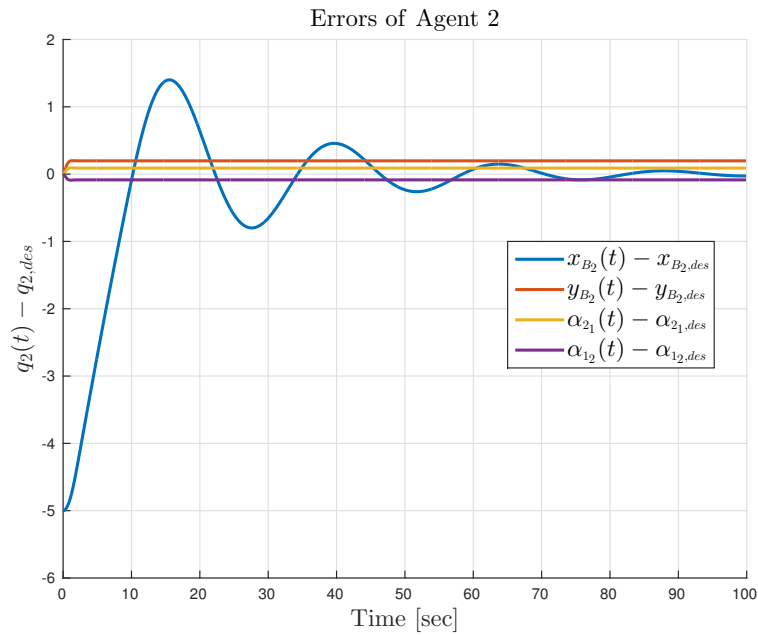


Fig. 12. The errors of vehicle 2 as well as the errors of the manipulator.

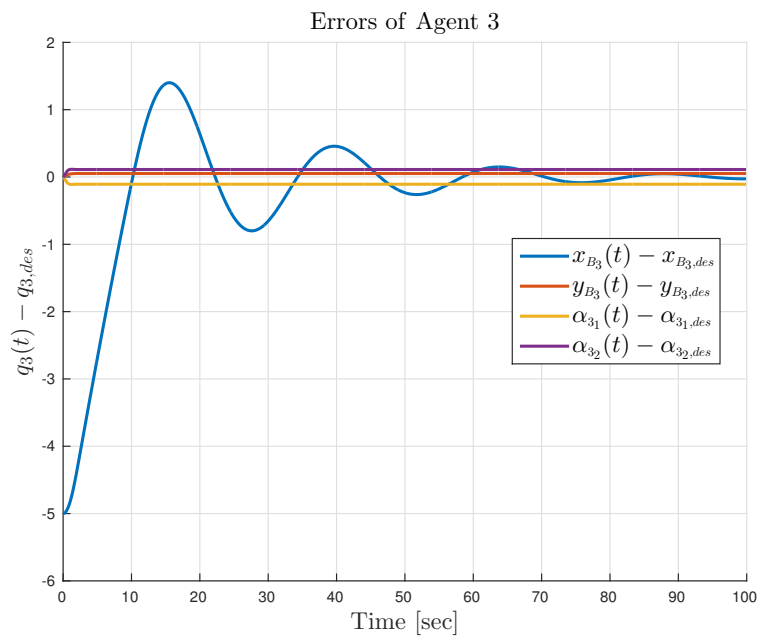


Fig. 13. The errors of vehicle 3 as well as the errors of the manipulator.

we have:

$$e^\top Q e + u^\top R u \leq \lambda_{\max}(Q) \|e\|^2 + \lambda_{\max}(R) \|u\|^2 = \max\{\lambda_{\max}(Q), \lambda_{\max}(R)\} \|z\|^2,$$

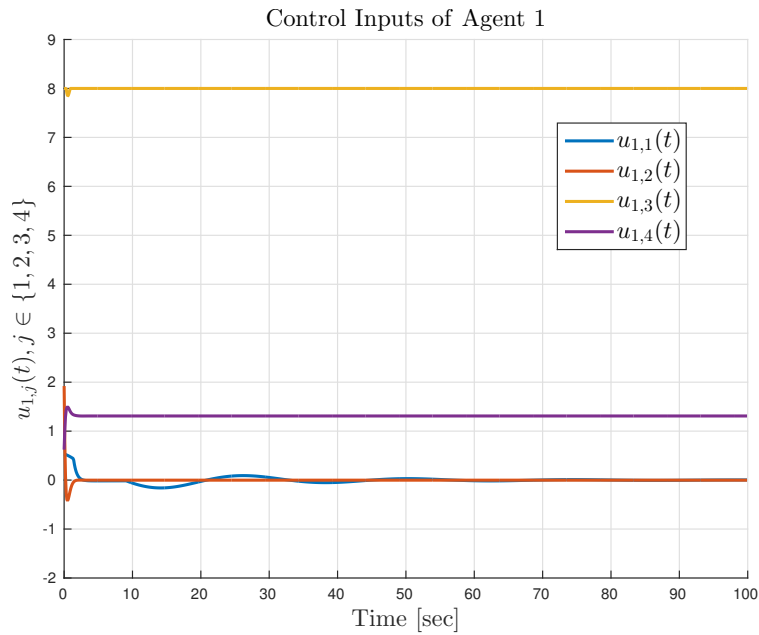


Fig. 14. The control inputs of the actuators of agent 1.

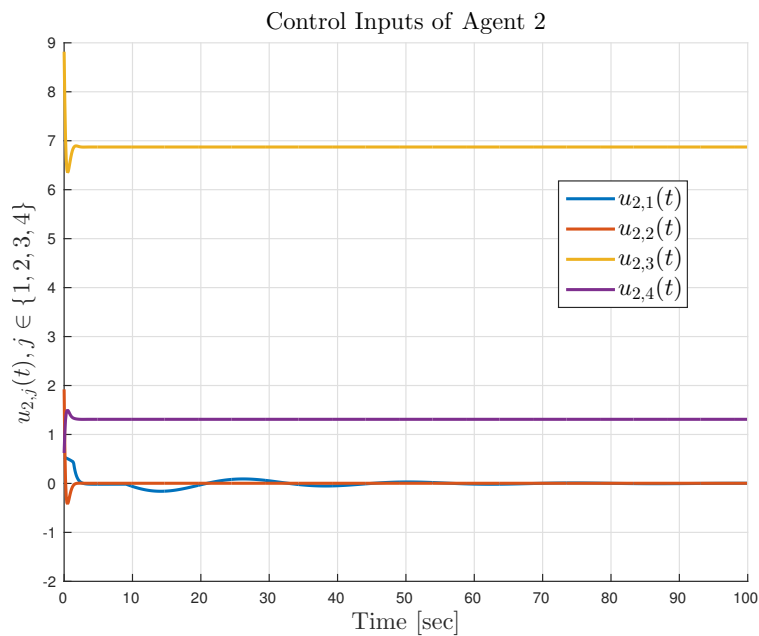


Fig. 15. The control inputs of the actuators of agent 3.

and:

$$\begin{aligned} e^\top Q e + u^\top R u &\geq \lambda_{\min}(Q) \|e\|^2 + \lambda_{\min}(R) \|u\|^2 \\ &= \min\{\lambda_{\min}(Q), \lambda_{\min}(R)\} \|z\|^2, \end{aligned}$$

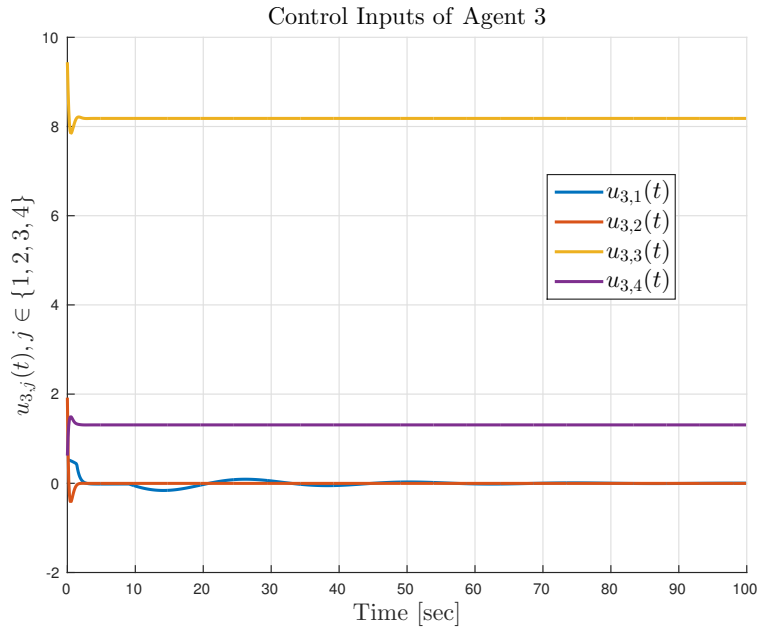


Fig. 16. The control inputs of the actuators of agent 3.

where $z = [e^\top, u^\top]^\top$. Thus, we get:

$$\min\{\lambda_{\min}(Q), \lambda_{\min}(R)\} \|z\|^2 \leq e^\top Q e + u^\top R u \leq \max\{\lambda_{\max}(Q), \lambda_{\max}(R)\} \|z\|^2.$$

By defining the \mathcal{K}_∞ functions $\alpha_1, \alpha_2 : \mathbb{R}_{\geq 0} \rightarrow \mathbb{R}_{\geq 0}$:

$$\alpha_1(y) \triangleq m \|y\|^2, \alpha_2(y) \triangleq \max\{\lambda_{\max}(Q), \lambda_{\max}(R)\} \|y\|^2,$$

and the parameter $m \in \mathbb{R}_{> 0}$ by:

$$m \triangleq \min\{\lambda_{\min}(Q), \lambda_{\min}(R)\}, \quad (27)$$

we get:

$$\alpha_1(\|z\|) \leq F(e, u) \leq \alpha_2(\|z\|), \quad (28)$$

which leads to the conclusion of the proof. \square

APPENDIX B
PROOF OF LEMMA 2

Proof. For every $e(t) \in \mathcal{E}_f$, the following holds:

$$\begin{aligned}
|V(e_1) - V(e_2)| &= |e_1^\top P e_1 - e_2^\top P e_2| \\
&= |e_1^\top P e_1 + e_1^\top P e_2 - e_1^\top P e_2 - e_2^\top P e_2| \\
&= |e_1^\top P(e_1 - e_2) - e_2^\top P(e_1 - e_2)| \\
&\leq |e_1^\top P(e_1 - e_2)| + |e_2^\top P(e_1 - e_2)|.
\end{aligned} \tag{29}$$

By employing the property that:

$$|x^\top A y| \leq \sigma_{\max}(A) \|x\| \|y\|, \forall x, y \in \mathbb{R}^n, A \in \mathbb{R}^{n \times n},$$

(29) is written as:

$$\begin{aligned}
|V(e_1) - V(e_2)| &\leq \sigma_{\max}(P) \|e_1\| \|e_1 - e_2\| + \sigma_{\max}(P) \|e_2\| \|e_1 - e_2\| \\
&= \sigma_{\max}(P) (\|e_1\| + \|e_2\|) \|e_1 - e_2\| \\
&\leq \sigma_{\max}(P) (\varepsilon_0 + \varepsilon_0) \|e_1 - e_2\| \\
&= [2\varepsilon_0 \sigma_{\max}(P)] \|e_1 - e_2\|.
\end{aligned}$$

which completes the proof. □

APPENDIX C
FEASIBILITY ANALYSIS

Consider any sampling time instant t_i for which a solution exists. In between t_i and t_{i+1} , the optimal control input $\hat{u}^*(s; e(t_i))$, $s \in [t_i, t_{i+1})$ is implemented. According to (25), it holds that:

$$e(t_{i+1}) = \hat{e}(t_{i+1}; \hat{u}^*(\cdot; e(t_i)), e(t_i)).$$

The remaining piece of the optimal control input $\hat{u}^*(s; e(t_i))$, $s \in [t_{i+1}, t_i + T_p]$ satisfies the state and input constraints E, U , respectively. Furthermore,

$$\hat{e}(t_i + T_p; \hat{u}^*(\cdot; e(t_i)), e(t_i)) \in \mathcal{E}_f,$$

and we know from Assumption 2b of Theorem 1 that for all $e(t) \in \mathcal{E}_f$, there exists at least one control input $u_f(\cdot)$ that renders the set \mathcal{E}_f invariant over h . Picking any such input, a feasible control input $\bar{u}(\cdot; e(t_{i+1}))$, at time instant t_{i+1} , may be the following:

$$\bar{u}(s; e(t_{i+1})) = \begin{cases} \hat{u}^*(s; e(t_i)), & s \in [t_{i+1}, t_i + T_p], \\ u_f(\hat{e}(t_i + T_p; u^*(\cdot), e(t_i))), & s \in [t_i + T_p, t_{i+1} + T_p]. \end{cases} \quad (30)$$

Thus, from feasibility of $\hat{u}^*(s, e(t_i))$ and the fact that $u_f(e(t)) \in U$, for all $e(t) \in \mathcal{E}_f$, it follows that:

$$\bar{u}(s; e(t_{i+1})) \in U, \forall s \in [t_{i+1}, t_i + T_p].$$

Hence, the feasibility at time t_i implies feasibility at time t_{i+1} . Therefore, if the OCP (21a) - (21d) is feasible at time $t = 0$, it remains feasible for every $t \geq 0$.

APPENDIX D CONVERGENCE ANALYSIS

The second part involves proving convergence of the state e in the terminal set \mathcal{E}_f . In order to prove this, it must be shown that a proper value function is decreasing along the solution trajectories starting at a sampling time t_i . Consider the optimal value function $J^*(e(t_i))$, as is given in (24). Consider also the cost of the feasible control input, indicated by:

$$\bar{J}(e(t_{i+1})) \triangleq \bar{J}(e(t_{i+1}), \bar{u}(\cdot; e(t_{i+1}))), \quad (31)$$

where $t_{i+1} = t_i + h$, as is given in (20). Define:

$$\begin{aligned} u_1(s) &= \bar{u}(s; e(t_{i+1})), \\ e_1(s) &= \bar{e}(s; u_1(s), e(t_{i+1})), s > t_{i+1}. \end{aligned} \quad (32)$$

$e_1(s)$ stands for the predicted state e at time s , based on the measurement of the state e at time t_{i+1} , while using the feasible control input $\bar{u}(s; e(t_{i+1}))$. Let us also define the following terms:

$$\begin{aligned} u_2(s) &= \hat{u}^*(s; e(t_i)), \\ e_2(s) &= \hat{e}(s; u_2(s), e(t_i)), s > t_{i+1}. \end{aligned} \quad (33)$$

(32), (33) form convenient notations for the readability of the proof hereafter.

By employing (21a), (24) and (31), the difference between the optimal and feasible cost is given by:

$$\begin{aligned}
\bar{J}(e(t_{i+1})) - J^*(e(t_i)) &= V(e_1(t_{i+1} + T_p)) + \int_{t_{i+1}}^{t_{i+1}+T_p} [F(e_1(s), u_1(s))] ds \\
&\quad - V(e_2(t_i + T_p)) - \int_{t_i}^{t_i+T_p} [F(e_2(s), u_2(s))] ds \\
&= V(e_1(t_{i+1} + T_p)) + \int_{t_{i+1}}^{t_i+T_p} [F(e_1(s), u_1(s))] ds \\
&\quad + \int_{t_i+T_p}^{t_{i+1}+T_p} [F(e_1(s), u_1(s))] ds - V(e_2(t_i + T_p)) \\
&\quad - \int_{t_i}^{t_{i+1}} [F(e_2(s), u_2(s))] ds - \int_{t_{i+1}}^{t_i+T_p} [F(e_2(s), u_2(s))] ds. \tag{34}
\end{aligned}$$

Note that, from (30), the following holds:

$$\bar{u}(s; e(t_{i+1})) = \hat{u}^*(s; e(t_i)), \forall s \in [t_{i+1}, t_i + T_p]. \tag{35}$$

By combining (32), (33) and (35), it yields that:

$$u_1(s) = u_2(s) = \bar{u}(s), \forall s \in [t_{i+1}, t_i + T_p], \tag{36}$$

which implies that:

$$e_1(s) = e_2(s), \forall s \in [t_{i+1}, t_i + T_p]. \tag{37}$$

The combination of (36) and (37) implies that:

$$F(e_1(s), u_1(s)) = F(e_2(s), u_2(s)), \forall s \in [t_{i+1}, t_i + T_p].$$

which implies that:

$$\int_{t_{i+1}}^{t_i+T_p} [F(e_1(s), u_1(s))] ds = \int_{t_{i+1}}^{t_i+T_p} [F(e_2(s), u_2(s))] ds. \tag{38}$$

By employing (38), (34) becomes:

$$\begin{aligned}
\bar{J}(e(t_{i+1})) - J^*(e(t_i)) &= V(e_1(t_{i+1} + T_p)) + \int_{t_i+T_p}^{t_{i+1}+T_p} [F(e_1(s), u_1(s))] ds \\
&\quad - V(e_2(t_i + T_p)) - \int_{t_i}^{t_{i+1}} [F(e_2(s), u_2(s))] ds. \tag{39}
\end{aligned}$$

Due to the fact that $t_{i+1} + T_p - (t_i + T_p) = t_{i+1} - t_i = h$, and the Assumption 2b of Theorem 1 holds for one sampling period h , by integrating this inequality from $t_i + T_p$ to $t_{i+1} + T_p$ and we get the following:

$$\begin{aligned}
& \int_{t_i+T_p}^{t_{i+1}+T_p} \left[\frac{\partial V}{\partial e} f_e(e_1(s), u_1(s)) + F(e_1(s), u_1(s)) \right] ds \leq 0 \\
\Leftrightarrow & \int_{t_i+T_p}^{t_{i+1}+T_p} \left[\dot{V}(e_1(s)) \right] ds + \int_{t_i+T_p}^{t_{i+1}+T_p} \left[F(e_1(s), u_1(s)) \right] ds \leq 0 \\
\Leftrightarrow & V(e_1(t_{i+1} + T_p)) - V(e_1(t_i + T_p)) + \int_{t_i+T_p}^{t_{i+1}+T_p} \left[F(e_1(s), u_1(s)) \right] ds \leq 0 \\
\Leftrightarrow & V(e_1(t_{i+1} + T_p)) - V(e_1(t_i + T_p)) + \int_{t_i+T_p}^{t_{i+1}+T_p} \left[F(e_1(s), u_1(s)) \right] ds \leq \\
& \quad V(e_2(t_i + T_p)) - V(e_2(t_i + T_p)) \\
\Leftrightarrow & V(e_1(t_{i+1} + T_p)) + \int_{t_i+T_p}^{t_{i+1}+T_p} \left[F(e_1(s), u_1(s)) \right] ds - V(e_2(t_i + T_p)) \leq \\
& \quad V(e_1(t_i + T_p)) - V(e_2(t_i + T_p)).
\end{aligned}$$

By employing the property $y \leq |y|, \forall y \in \mathbb{R}$, we get:

$$\begin{aligned}
& V(e_1(t_{i+1} + T_p)) + \int_{t_i+T_p}^{t_{i+1}+T_p} \left[F(e_1(s), u_1(s)) \right] ds - V(e_2(t_i + T_p)) \leq \\
& \quad |V(e_1(t_i + T_p)) - V(e_2(t_i + T_p))|.
\end{aligned} \tag{40}$$

By employing Lemma 2, we have that:

$$|V(e_1(t_i + T_p)) - V(e_2(t_i + T_p))| \leq L_V \|e_1(t_i + T_p) - e_2(t_i + T_p)\|. \tag{41}$$

By combining (40) and (41) we get:

$$\begin{aligned}
& V(e_1(t_{i+1} + T_p)) + \int_{t_i+T_p}^{t_{i+1}+T_p} \left[F(e_1(s), u_1(s)) \right] ds - V(e_2(t_i + T_p)) \leq \\
& \quad L_V \|e_1(t_i + T_p) - e_2(t_i + T_p)\|
\end{aligned} \tag{42}$$

For $s = t_i + T_p$, (37) gives:

$$e_1(t_i + T_p) = e_2(t_i + T_p). \tag{43}$$

By combining (43) and (42) we have:

$$\begin{aligned}
& V(e_1(t_{i+1} + T_p)) + \\
& \quad \int_{t_i+T_p}^{t_{i+1}+T_p} \left[F(e_1(s), u_1(s)) \right] ds - V(e_2(t_i + T_p)) \leq 0.
\end{aligned} \tag{44}$$

By combining (39) with (44), the following holds:

$$\bar{J}(e(t_{i+1})) - J^*(e(t_i)) \leq - \int_{t_i}^{t_{i+1}} \left[F(e_2(s), u_2(s)) \right] ds. \quad (45)$$

By substituting $e = e_2(s), u = u_2(s)$ in (28) we get:

$$F(e_2(s), u_2(s)) \geq m \|z_2(s)\|^2,$$

where $z_2 \triangleq [e_2, u_2]^\top$. The latter is equivalent to:

$$\begin{aligned} \int_{t_i}^{t_{i+1}} \left[F(e_2(s), u_2(s)) \right] ds &\geq m \int_{t_i}^{t_{i+1}} \|z_2(s)\|^2 ds \\ \Leftrightarrow - \int_{t_i}^{t_{i+1}} \left[F(e_2(s), u_2(s)) \right] ds &\leq -m \int_{t_i}^{t_{i+1}} \|z_2(s)\|^2 ds. \end{aligned} \quad (46)$$

By combining (45) and (46) we finally get:

$$\bar{J}(e(t_{i+1})) - J^*(e(t_i)) \leq -m \int_{t_i}^{t_{i+1}} \|z_2(s)\|^2 ds. \quad (47)$$

It is clear that the optimal solution at time t_{i+1} i.e., $J^*(e(t_{i+1}))$ will not be worse than the feasible one at the same time i.e. $\bar{J}(e(t_{i+1}))$. Therefore, (47) implies:

$$J^*(e(t_{i+1})) - J^*(e(t_i)) \leq -m \int_{t_i}^{t_{i+1}} \|z_2(s)\|^2 ds \leq 0, \quad (48)$$

or, by using the fact that $\int_{t_0}^{t_i} \|z_2(s)\|^2 ds = \sum_{j=0}^{i-1} \int_{t_j}^{t_{j+1}} \|z_2(s)\|^2 ds$, equivalently, we obtain:

$$J^*(e(t_{i+1})) - J^*(e(t_i)) \leq -m \int_{t_0}^{t_{i+1}} \|z_2(s)\|^2 ds + m \sum_{j=0}^{i-1} \int_{t_j}^{t_{j+1}} \|z_2(s)\|^2 ds. \quad (49)$$

By using induction and the fact that $t_i = h \cdot i, t_{i+1} = h \cdot (i+1), \forall i \geq 0$, from (20), (49) is written as:

$$J^*(e(t_i)) - J^*(e(t_0)) \leq -m \int_{t_0}^{t_i} \|z_2(s)\|^2 ds. \quad (50)$$

Since $t_0 = 0$ we obtain:

$$J^*(e(t_i)) \leq J^*(e(0)) - m \int_0^{t_i} \|z_2(s)\|^2 ds. \quad (51)$$

which implies that:

$$J^*(e(t_i)) \leq J^*(e(0)). \quad (52)$$

By combining (48), (52), we obtain:

$$J^*(e(t_{i+1})) \leq J^*(e(t_i)) \leq J^*(e(0)), \forall t_i = i \cdot h, i \geq 0. \quad (53)$$

Therefore, the value function $J^*(e(t_i))$ has proven to be non-increasing for all the sampling times. Let us define the function:

$$V(e(t)) = J^*(e(s)) \leq J^*(e(0)), t \in \mathbb{R}_{\geq 0}, \quad (54)$$

where $s = \max\{t_i : t_i \leq t\}$. Since $J^*(e(0))$ is bounded, (54) implies that $V(e(t))$ is bounded. Since the signals $e(t), u(t)$ are bounded ($e(t) \in E, u(t) \in U$), according to (16), it holds that $\dot{e}(t)$ is also bounded. From (51) we have that:

$$V(e(t)) = J^*(e(s)) \leq J^*(e(0)) - m \int_0^s \|z_2(s)\|^2 ds.$$

which due to the fact that $s \leq t$, is equivalent to:

$$V(e(t)) \leq J^*(e(0)) - m \int_0^t \|z_2(s)\|^2 ds, t \in \mathbb{R}_{\geq 0}. \quad (55)$$

From (55), we get:

$$\int_0^t \|z_2(s)\|^2 ds \leq \frac{1}{m} [J^*(e(0)) - V(e(t))], t \in \mathbb{R}_{\geq 0}. \quad (56)$$

Since $J^*(e(0)), V(e(t))$ has been proven to be bounded, the term $\int_0^t \|z_2(s)\|^2 ds$ is also bounded. Therefore, by employing Lemma 1, we have that $\|z_2(t)\| \rightarrow 0$, as $t \rightarrow \infty$. The latter implies that:

$$\lim_{t \rightarrow \infty} \|e(t)\| = 0 \Rightarrow e(t) \in \mathcal{E}_f, \text{ as } t \rightarrow \infty,$$

and leads to the conclusion of the proof.

REFERENCES

- [1] S. A. Schneider and R. H. Cannon, "Object impedance control for cooperative manipulation: Theory and experimental results," *IEEE Transactions on Robotics and Automation*, vol. 8, no. 3, pp. 383–394, 1992.
- [2] Y.-H. Liu, S. Arimoto, and T. Ogasawara, "Decentralized cooperation control: non-communication object handling," *Proceedings of the IEEE Conference on Robotics and Automation (ICRA)*, vol. 3, pp. 2414–2419, 1996.
- [3] Y.-H. Liu and S. Arimoto, "Decentralized adaptive and nonadaptive position/force controllers for redundant manipulators in cooperations," *The International Journal of Robotics Research*, vol. 17, no. 3, pp. 232–247, 1998.
- [4] M. Zribi and S. Ahmad, "Adaptive control for multiple cooperative robot arms," *Proceedings of the IEEE International Conference on Decision and Control (CDC)*, pp. 1392–1398, 1992.
- [5] O. Khatib, K. Yokoi, K. Chang, D. Ruspini, R. Holmberg, and A. Casal, "Decentralized cooperation between multiple manipulators," *IEEE International Workshop on Robot and Human Communication*, pp. 183–188, 1996.
- [6] F. Caccavale, P. Chiacchio, and S. Chiaverini, "Task-space regulation of cooperative manipulators," *Automatica*, vol. 36, no. 6, pp. 879–887, 2000.

- [7] J. Gudiño-Lau, M. A. Arteaga, L. A. Munoz, and V. Parra-Vega, “On the control of cooperative robots without velocity measurements,” *IEEE Transactions on Control Systems Technology*, vol. 12, no. 4, pp. 600–608, 2004.
- [8] F. Caccavale, P. Chiacchio, A. Marino, and L. Villani, “Six-dof impedance control of dual-arm cooperative manipulators,” *IEEE/ASME Transactions On Mechatronics*, vol. 13, no. 5, pp. 576–586, 2008.
- [9] D. Heck, D. Kostić, A. Denasi, and H. Nijmeijer, “Internal and external force-based impedance control for cooperative manipulation,” *Proceedings of the IEEE European Control Conference (ECC)*, pp. 2299–2304, 2013.
- [10] S. Erhart and S. Hirche, “Adaptive force/velocity control for multi-robot cooperative manipulation under uncertain kinematic parameters,” *Proceedings of the IEEE/RSJ International Conference on Intelligent Robots and Systems (IROS)*, pp. 307–314, 2013.
- [11] S. Erhart, D. Sieber, and S. Hirche, “An impedance-based control architecture for multi-robot cooperative dual-arm mobile manipulation,” *Proceedings of the IEEE/RSJ International Conference on Intelligent Robots and Systems (IROS)*, pp. 315–322, 2013.
- [12] J. Szewczyk, F. Plumet, and P. Bidaud, “Planning and controlling cooperating robots through distributed impedance,” *Journal of Robotic Systems*, vol. 19, no. 6, pp. 283–297, 2002.
- [13] A. Tsiamis, C. K. Verginis, C. P. Bechlioulis, and K. J. Kyriakopoulos, “Cooperative manipulation exploiting only implicit communication,” *Proceedings of the IEEE/RSJ International Conference on Intelligent Robots and Systems (IROS)*, pp. 864–869, 2015.
- [14] F. Ficuciello, A. Romano, L. Villani, and B. Siciliano, “Cartesian impedance control of redundant manipulators for human-robot co-manipulation,” *Proceedings of the IEEE/RSJ International Conference on Intelligent Robots and Systems (IROS)*, pp. 2120–2125, 2014.
- [15] A. Ponce-Hinestroza, J. Castro-Castro, H. Guerrero-Reyes, V. Parra-Vega, and E. Olguyn-Dyaz, “Cooperative redundant omnidirectional mobile manipulators: Model-free decentralized integral sliding modes and passive velocity fields,” *Proceedings of the IEEE International Conference on Robotics and Automation (ICRA)*, pp. 2375–2380, 2016.
- [16] W. Gueaieb, F. Karray, and S. Al-Sharhan, “A robust hybrid intelligent position/force control scheme for cooperative manipulators,” *IEEE/ASME Transactions on Mechatronics*, vol. 12, no. 2, pp. 109–125, 2007.
- [17] M. Ciocarlie, F. M. Hicks, R. Holmberg, J. Hawke, M. Schlicht, J. Gee, S. Stanford, and R. Bahadur, “The velo gripper: A versatile single-actuator design for enveloping, parallel and fingertip grasps,” *The International Journal of Robotics Research*, 2014.
- [18] D. E. Koditschek and E. Rimon, “Robot navigation functions on manifolds with boundary,” *Advances in applied mathematics*, vol. 11, no. 4, pp. 412–442, 1990.
- [19] B. Siciliano, L. Sciavicco, and L. Villani, “*Robotics: Modelling, Planning and Control*”. Advanced Textbooks in Control and Signal Processing, Springer, 2009.
- [20] K. S. de Oliveira and M. Morari, “Contractive Model Predictive Control for Constrained Nonlinear Systems,” *IEEE Transactions on Automatic Control*, vol. 45, no. 6, pp. 1053–1071, 2000.
- [21] R. Findeisen, L. Imsland, F. Allgower, and B. A. Foss, “State and Output Feedback Nonlinear Model Predictive Control: An Overview,” *European Journal of Control*, vol. 9, no. 2-3, pp. 190–206, 2003.
- [22] H. Chen and F. Allgöwer, “A Quasi-Infinite Horizon Nonlinear Model Predictive Control Scheme with Guaranteed Stability,” *Automatica*, vol. 34, no. 10, pp. 1205–1217, 1998.
- [23] R. Findeisen, L. Imsland, F. Allgöwer, and B. Foss, “Towards a Sampled-Data Theory for Nonlinear Model Predictive Control,” *New Trends in Nonlinear Dynamics and Control and their Applications*, pp. 295–311, 2003.
- [24] F. Fontes, “A General Framework to Design Stabilizing Nonlinear Model Predictive Controllers,” *Systems and Control Letters*, vol. 42, no. 2, pp. 127–143, 2001.

- [25] L. Grüne and J. Pannek, *Nonlinear Model Predictive Control*. Springer London, 2011.
- [26] E. Camacho and C. Bordons, “Nonlinear Model Predictive Control: An Introductory Review,” pp. 1–16, 2007.
- [27] B. Kouvaritakis and M. Cannon, *Nonlinear Predictive Control: Theory and Practice*. No. 61, Iet, 2001.
- [28] J. Frasch, A. Gray, M. Zanon, H. Ferreau, S. Sager, F. Borrelli, and M. Diehl, “An Auto-Generated Nonlinear MPC Algorithm for Real-Time Obstacle Cvoidance of Ground Vehicles,” *European Control Conference (ECC)*, 2013.
- [29] F. Fontes, L. Magni, and É. Gyurkovics, “Sampled-Data Model Predictive Control for Nonlinear Time-Varying Systems: Stability and Robustness,” *Assessment and Future Directions of Nonlinear Model Predictive Control*, pp. 115–129, 2007.
- [30] A. Nikou, C. K. Verginis, S. Heshmati-alamdari, and D. V. Dimarogonas, “A Nonlinear Model Predictive Control Scheme for Cooperative Manipulation with Singularity and Collision Avoidance,” *25th IEEE Mediterranean Conference on Control and Automation (MED)*, Valletta, Malta, 2017.
- [31] A. Nikou, S. Heshmati-alamdari, C. K. Verginis, and D. V. Dimarogonas, “Decentralized Abstractions and Timed Constrained Planning of a General Class of Coupled Multi-Agent Systems,” *56th IEEE Conference on Decision and Control (CDC)*, *ArXiv Link: <https://arxiv.org/abs/1703.06070>*, 2017.
- [32] A. Filotheou, A. Nikou, and D. V. Dimarogonas, “Decentralized Control of Uncertain Multi-Agent Systems with Connectivity Maintenance and Collision Avoidance,” *IEEE European Control Conference (ECC)*, *Under Review*, *ArXiv Link: <https://arxiv.org/abs/1710.09204>*, 2017.
- [33] A. Filotheou, A. Nikou, and D. Dimarogonas, “Robust Decentralized Navigation of Multiple Rigid Bodies with Collision Avoidance and Connectivity Maintenance Using Model Predictive Controllers,” *International Journal of Control (IJC)*, *Under Review*, 2017.
- [34] C. K. Verginis, A. Nikou, and D. Dimarogonas, “Communication-based Decentralized Cooperative Object Transportation Using Nonlinear Model Predictive Control,” *IEEE European Control Conference (ECC)*, *Under Review*, 2017.
- [35] H. Khalil, *Nonlinear Systems*. Prentice-Hall, New Jersey, 1996.
- [36] H. Michalska and R. Vinter, “Nonlinear Stabilization Using Discontinuous Moving-Horizon Control,” *IMA Journal of Mathematical Control and Information*, vol. 11, no. 4, pp. 321–340, 1994.